European Polymer Journal 44 (2008) 2838–2844

Contents lists available at ScienceDirect

European Polymer Journal

journal homepage: www.elsevier.com/locate/europolj

Macromolecular Nanotechnology

Production of aligned helical polymer nanofibers by electrospinning

Jie Yu [a,*], Yejun Qiu [a], Xiaoxiong Zha [b,*], Min Yu [b], Jiliang Yu [b], Javed Rafique [a], Jing Yin [b]

[a] Department of Materials Science and Engineering, Shenzhen Graduate School, Harbin Institute of Technology, University Town, Xili, Shenzhen 518055, China
[b] Structural and Geotechnical Engineering Research Center (SGERC), Shenzhen Graduate School, Harbin Institute of Technology, University Town, Xili, Shenzhen 518055, China

ARTICLE INFO

Article history:
Received 9 January 2008
Received in revised form 23 April 2008
Accepted 22 May 2008
Available online 2 June 2008

Keywords:
Electrospinning
Alignment
Helical nanofibers
Polycaprolactone
Concentration

ABSTRACT

A new and simple electrospinning method has been developed for producing aligned helical polymer nanofibers. Aligned helical polycaprolactone (PCL) nanofibers were prepared by this method. The helical fibers were collected by a tilted glass slide. The morphology and loop diameters of the helical structures are dependant on the PCL solution concentration and the loop diameters are in the range of 6.9–14.9 μm for the concentration range of 4.7%–10%. The three-dimensional helical structures were obtained at the high solution concentration of 10%. These helical structures were formed by jet buckling due to mechanical instability when hitting collector surface. Formation of the helical structures is dependent on the obliquity of the tilted glass slide and distance away from the syringe needle. The converging electrical field generated by a tip collector plays an important role in the alignment of the helical structures.

1. Introduction

Helical structures at micro- and nano-scale are of great interest due to their potential applications as structural and inductive components in micro- and nano-electromechanical systems and electromagnetic systems, composite materials, advanced optical components, and drug delivery system and other biomaterials. For example, an inductive magnetic field could be generated while an electrical current flows through helical carbon nanotubes, which implies that the helical carbon nanotubes may be used as electromagnetic nano-transformers or nano-switches [1]. In addition, the helical structures are the most fundamental configuration for biomolecules such as proteins, DNA, and starch. Even more, the bodies of some microorganisms such as spirilla and helical algae are helical. By using vapor phase growth processes some helical nanostructures of inorganic materials such as carbon [1], SiO_2 [2], and ZnO [3] have been prepared. Recently, helical polymeric nanofibers with loop diameter in the range of several to over 20 μm have been prepared by electrospinning [4–7]. Kessick et al. produced helical nanofibers of a composite containing one conducting and one nonconducting polymer on conducting substrates [4]. It was proposed that partial viscoelastic contraction caused by partial charge neutralization mainly on the conductive phase is responsible for the formation of the helical structures. Shin et al fabricated single-phase nonconducting helical polymeric nanofibers of poly(2-acrylamido-2-methyl-1-propanesulfonic acid). They indicated that physical forces caused by the bending instability of the jet played an important role in the formation of the helical structures [5]. Xin et al. prepared poly(*p*-phenylene vinylene)/poly(vinyl pyrrolidone) composite nanofibers with helical structure [6]. They considered that the viscosity and conductivity of the electrospinning solutions and the operating voltage are the main factors affecting the formation of the helical structures. Lin et al. fabricated side-by-side bicomponent helical nanofibers with coil diameters as small as 500 nm, the helices were formed driven by the difference in shrinkage between the two components [7]. More recently, the in-depth study by Reneker et al. demonstrated that the helical structures

* Corresponding authors. Tel.: +86 755 26033478; fax: +86 755 26033504.
E-mail addresses: msejyu@yahoo.com, jyu@hitsz.edu.cn (J. Yu), zhaxx@hit.edu.cn (X. Zha).

0014-3057/$ - see front matter © 2008 Elsevier Ltd. All rights reserved.
doi:10.1016/j.eurpolymj.2008.05.020

at micro-scale were formed by buckling occurred when the jet was stopped on the collector during electrospinning [8].

However, production of the helical polymer nanofibers in a controllable process at low cost is still a challenge so far. The fibers are generally collected in the form of randomly oriented mats due to the bending instability of the highly charged jet [9] for conventional electrospinning process. However, well-aligned and highly ordered architectures are often required in most applications both for straight and helical polymer nanofibers. Considerable success has been achieved in controlling the spatial orientation of the straight polymer fibers by both mechanically moving the collectors and electrostatic inducement [10–18]. But it is still an open question to fabricate aligned helical polymer nanofibers by electrospinning up to now. In this work, a simple electrospinning approach was developed, by which the aligned helical polycaprolactone (PCL) nanofibers were readily fabricated. The helical structures were formed by jet buckling when hitting the collector surface during electrospinning.

2. Experimental

PCL (Mw = 150000) was purchased from Aldrich. *N*, *N*-dimethyleformamide (DMF) was purchased from Shantou Xilong Chemical Company and tetrahydrofuran (THF) was purchased from Tianjin Damao Chemical Reagent Factory. All the chemicals were used as received without any purification. A high voltage power supply (DW-P503-2AC, 0 V ~ +50 kV) was used during the experiments. The morphology of the fibers was characterized by a Union-DZ3 optical microscope and scanning electron microscopy (SEM) (Hitachi S-4700). A Magnetic stirrer was used for stirring the solution. Hypodermic plastic syringes were used to hold the polymer solution and the syringe needle was 0.65 mm in inner diameter. The PCL nanofibers were collected by a glass slide of 75 × 25 mm^2 in size. During all the experiments the positive terminal (copper wire) of the power supply was dipped in the polymer solution and the ground electrode was used as the collector. No syringe pump was used for all the experiments. PCL solutions from 3.5% to 10% in THF: DMF (1:1) were prepared under 24 h magnetic stirring. The nanofiber samples were electrospun at the voltage of 18 kV.

3. Results and discussion

Fig. 1 shows a schematic of our electrospinning setup, by which we have prepared highly aligned straight polymer nanofibers on large scale [19]. Different from the conventional electrospinning setup, the grounded collector electrode (1) here is a metal wire only 2 mm in diameter, fixed in a hole centered at a wooden board (2). This collector was named 'tip collector' due to the small size [19]. The ground electrode (1) is placed at an angular distance from the syringe nozzle, rather than just below it. A tilted glass slide (3) located between the ground electrode and the syringe needle was used for collecting the helical fibers. In the figure, h is the height difference between the ground electrode tip and the syringe needle tip, θ is the angle between

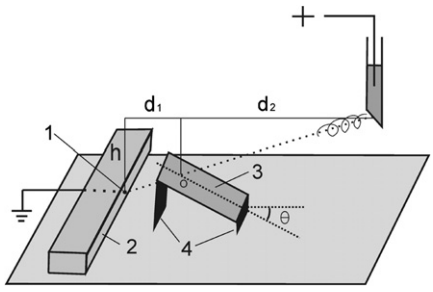

Fig. 1. Schematic of the electrospinning setup. 1-grounded electrode wire, 2-wooden board, 3-glass slide, 4-supporter.

the glass slide surface and the horizontal plane, dot O is the intersecting point between the glass slide surface and the straight line connecting the syringe needle tip and the ground electrode tip, d_1 and d_2 are the horizontal distances from O to the ground electrode tip and needle tip, respectively. In our experiments $d_1 + d_2$ of 12 cm and h of 3.5 cm were used.

Fig. 2 shows the optical images of the PCL fibers electrospun for about 20 s at the concentration (weight ratio) of 3.5%, 4.7%, 5.8%, 6.8%, and 10%, respectively. These fibers were collected on the glass slide located at d_1 of 1 cm and θ of 20°. Apart from the fibers electrospun from the solution of concentration 3.5% shown in Fig. 2A, the helical structures were observed for all the other samples (Fig. 2B–E), where the loop diameters of the helical structures are several to over 10 μm, much smaller than the loop diameters of several millimeters to centimeters for the cone helix produced by the electrical bending instability [8,9]. Obviously, these helical structures did not originate from the electrical bending instability, but from the mechanical buckling instability occurred when the jets impinged on the collector surface according to Reneker [8]. In the electrospinning process, the jet was in compression as it encountered the collector surface, and thus the buckling instability resulted. The buckling instability induced the fibers to form sinuous folding, zigzag folding or helical folding structure. In the present work, the fiber morphology changed from the sinuous folding at the solution concentration of 3.5% to the helical coiling at the concentration of 4.7% and above. It was found that the formation of the aligned helical structures and their alignment were greatly dependent on the location and slope of the glass slides. The helical PCL nanofibers were generally obtained for θ in the range of 0–45° and d_1 of 0–6 cm. The optimal range of θ was found to be 10–30°; within this range the helical structures were better developed and predominant in the products. No obvious changes were observed with changing the tilting angle of the glass slide in this range. When collecting at $d_2 < 5$ cm the fibers tended to accumulate together in small area. And the fibers tended to be straight when $\theta > 45°$ even at the location of d_1 in the range of 0–6 cm. Fig. 3A and B show the optical images of the helical polymer nanofibers deposited for 10 s and 40 s, respectively. It is indicated that the coiling structure and alignment changed not much with increasing the deposition time. By depositing for short time the micro patterns of

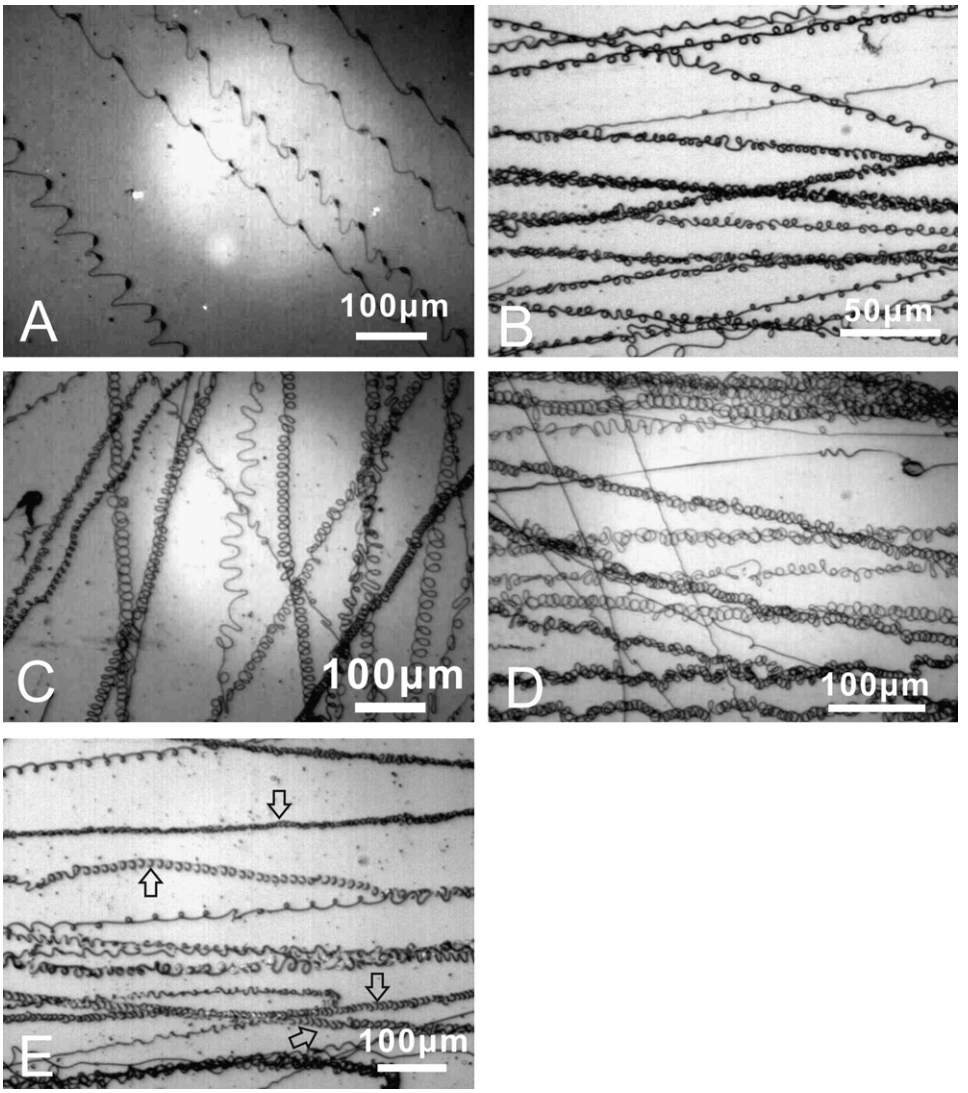

Fig. 2. Optical images of the PCL fibers prepared at different solution concentration: (A) 3.5%, (B) 4.7%, (C) 5.8%, (D) 6.8%, (E) 10%.

the helical fibers can be obtained, and by depositing for long time the polymer films composed of the helical fibers can be obtained.

During the experiments, we clearly found that the loop diameter of the helical structures changes with solution concentration. The dependence of the average loop diameter on the solution concentration is shown in Fig. 4, which indicates that the loop diameter increases with increasing the solution concentration initially and then decreases with further increasing the concentration after reaching the largest diameter of 14.9 μm at the concentration of 5.8%. The same trend was also observed in electrospinnig the helical fibers of composite containing poly(ethylene oxide) (PEO) and poly(aniline sulfonic acid), where the largest coil diameter was obtained at the PEO concentration of 8.5% [4]. The mechanism of this changing trend in loop diameter with solution concentration is not clear for us at present.

The morphology of the PCL fibers changes with the solution concentration. At the low concentration of 3.5%, the PCL nanofibers has the morphology of beads-on-string, which was commonly observed for the low concentration electrospinning due to the relatively low viscosity and high surface tension [20,21]. With increasing the solution concentration to 4.7% and above, the beads disappeared and the helical nanofibers were obtained. Interestingly, some three-dimensional (3-D) helical nanofibers were obtained at the solution concentration of 10% as marked by the arrows in Fig. 2E. Generally, the helical structures prepared by electrospinning are two-dimensional (2-D), i.e. the fibers coiled only within the collector surface. Fig. 5A and B show the enlarged images of the 3-D and 2-D helical nanofibers, respectively. The difference between them can be clearly observed. The 3-D helical structures are real micro-springs and may find applications in micro-electro-mechanical systems.

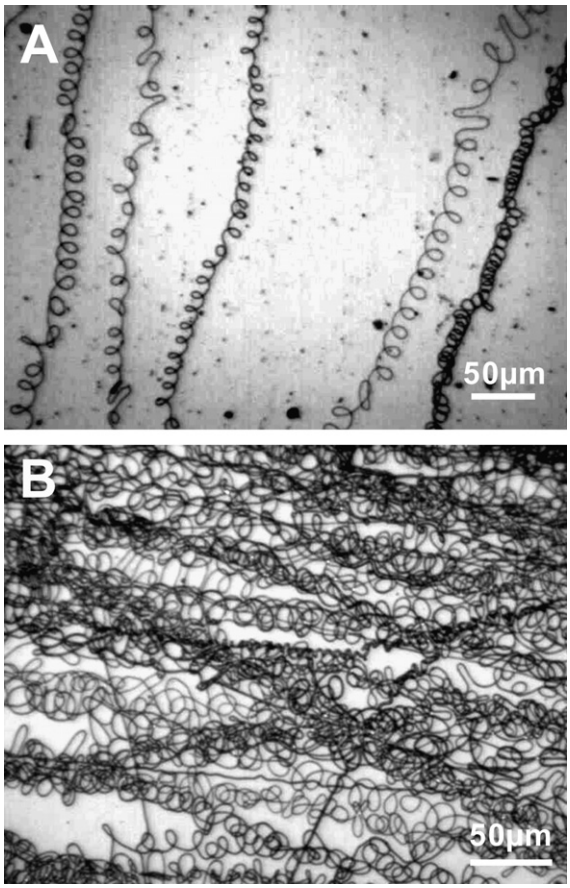

Fig. 3. Optical images of the helical PCL fibers deposited for different time. (A) 10 s, (B) 40 s.

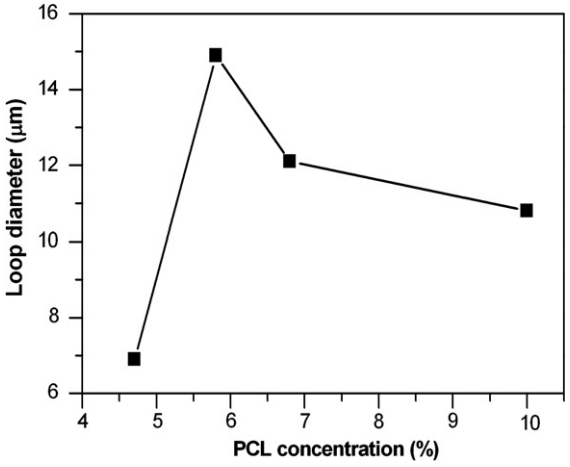

Fig. 4. Loop diameters of the PCL helical structures versus solution concentration.

The detailed formation mechanism of the helical structures during electrospinning is not clear in the present stage and we can only tentatively give some explanations based on the obtained results. We found that formation

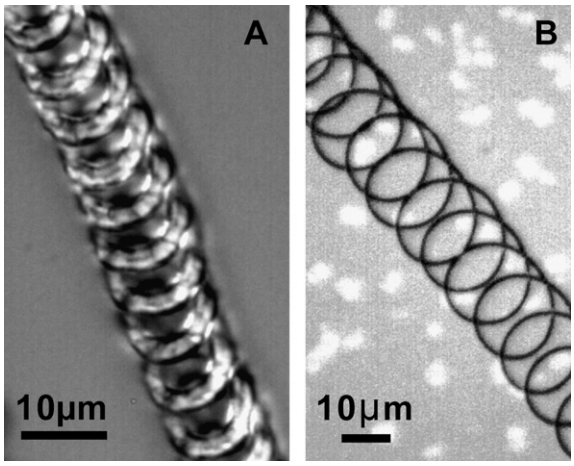

Fig. 5. Optical images of the 3-D (A) and 2-D (B) PCL helical structures.

behavior of the helical structures was obviously dependant on the solution concentration with other process parameters such as tilting angle of the glass slide constant. As shown above, the helical structures can only form at the concentration of 4.7% and above while at the low solution concentration of 3.5% almost no helical structures were observed. Furthermore, at the high concentration of 10% formation of the 3-D helical structures was observed. It is thus inferred that formation of the helical structures is closely related to viscosity of the solution and stiffness of the jets. It has been known that buckling instability of jets impinging on substrate surface induced formation of the helical structures. The morphology of the collected fibers should be dependant on the mode of the buckling instability. The driven force of buckling is the compressive stress generated in the jets when impinging on substrate surface [8]. Some stiffness is thus required for the jets to generate stress for supporting the buckling. As indicated by Reneker [8], buckling occurs only when the jets are solid enough. At the low concentration of 3.5% the jets are too fluid to generate enough high stress for supporting their movement along spiral routes in relative large area to form spiral shape during buckling, and thus only sinuous folding structure formed. With increasing solution concentration the jets became more solid, resulting in the formation of the helical structures. The formation of the 3-D helical structures at the solution concentration of 10% is because the jets are solid enough to support themselves suspending in air at this concentration. However, formation of the helical structures depends not only on the solution concentration but also the incident angle of the jets. As indicated above, almost no helical fibers formed if the tilting angle of the glass slide is over 45° even at identical solution concentration. We noticed that the sinuous or straight fibers were also generated along with the helical fibers as shown in Fig. 2B–D and the 2-D and 3-D helical structures were formed simultaneously as shown in Fig. 2E. We believe that this is mainly because the incident angle was different for these jets. Although most of the jets are aligned during flight by the converging electrical field the angles they impinged on the glass surface are not strictly identical to each

other and sometimes quite different due to the whipping instability and disturbance from environmental airflow etc. The mode of buckling instability is at least partially dependant on the incident angle. It is estimated that the fibers tend to be sinuous or straight if the incident angle is too small. The concurrent formation of the 2-D and 3-D structures may be also attributed to the different incident angles of the jets; but the specific formation mechanism is inaccessible to us now.

In order to determine the diameters of the electrospun fibers SEM images were taken at higher magnification. Fig. 6A–C show the typical SEM images of the electrospun fibers at the solution concentrations of 3.5%, 5.8%, and 10%, respectively, corresponding to the samples shown in Fig. 2A, C and E. The diameter of the fibers electrospun at the concentration of 3.5%, 5.8%, and 10% falls in the range of 150–250 nm, 200–400 nm, and 1.2–2 μm, respectively. It is indicated that the diameter of the electrospun fibers increases with increasing the solution concentration.

In conventional electrospinning process the fibers are ejected continuously, where one end of the fiber is fixed at the needle tip. In the present case, it is inferred that the fibers are electrospun individually and one by one due to the low solution flow rate from the syringe reservoir to needle tip, which is supported by the real time images presented in our previous paper [19]. This is mainly because the syringe pumps were not used during electrospinning and the solution flow from the syringe reservoir to the needle tip was only driven by gravitation. In the case of low solution flow rate, once a droplet was exhausted a single fiber with two free ends formed. According to the reported calculation results [11], the electrical field generated by the tip electrode is converging towards the electrode tip. We also calculated the difference between the electrical fields generated by a tip electrode and a large area electrode. The syringe needle was simplified to be a point charge during calculation. Fig. 7A shows the equipotential lines and the electrical field lines between the collector (ground electrode) and syringe needle (point charge) by assuming the collector size to be $40 \times 40\ cm^2$ and Fig. 7B is that by assuming the collector size to be $2 \times 2\ mm^2$. It is clearly observed that the electrical field lines are almost parallel to each other near the large collector, whereas the field lines are converging in the case of small collector electrode. As a consequence, the front end of the ejected fiber is dragged towards the collector tip by the converging electrical field, which tends to direct the fiber flight with its axis in parallel to the line connecting the needle tip and electrode tip. In conjunction with the repelling force from the formerly deposited helical fibers with charge, alignment is achieved on the glass slides for all the helical nanofibers. In order to know the influence of the glass slide the electrical field distribution was also calculated by considering the existence of the glass slide. Fig. 7C shows the equipotential lines and electrical field lines in the existence of the glass slide with other parameters identical to that of Fig. 7B. The size of $1 \times 25 \times 75\ mm^3$, dielectric constant of 8, and location of 1 cm away from the collector electrode were adopted during calculation. It is clearly indicated that the electrical field distribution is still converging towards the collector and no visible changes were observed in despite of introduction of the glass slide. Similar to the alignment mechanism of the straight fibers shown in Ref. [19], the alignment of the helical fibers in this work was also achieved by the converging electrical field. As stated in Ref. [19], the jets were aligned mainly during flight from needle to collector. By introducing a titled glass slide the jets already aligned during flight became helical due to buckling instability. The detailed alignment mechanism was presented elsewhere [19]. Further work is underway

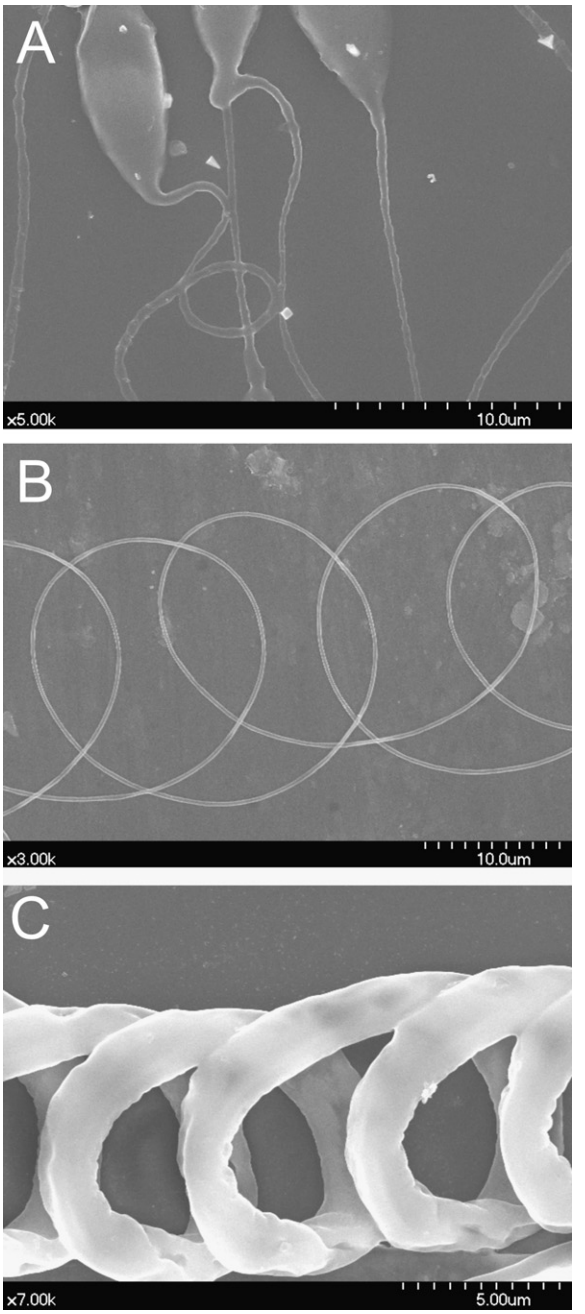

Fig. 6. SEM images of the PCL fibers electrospun at different solution concentration: (A) 3.5%, (B) 5.8%, (C) 10%.

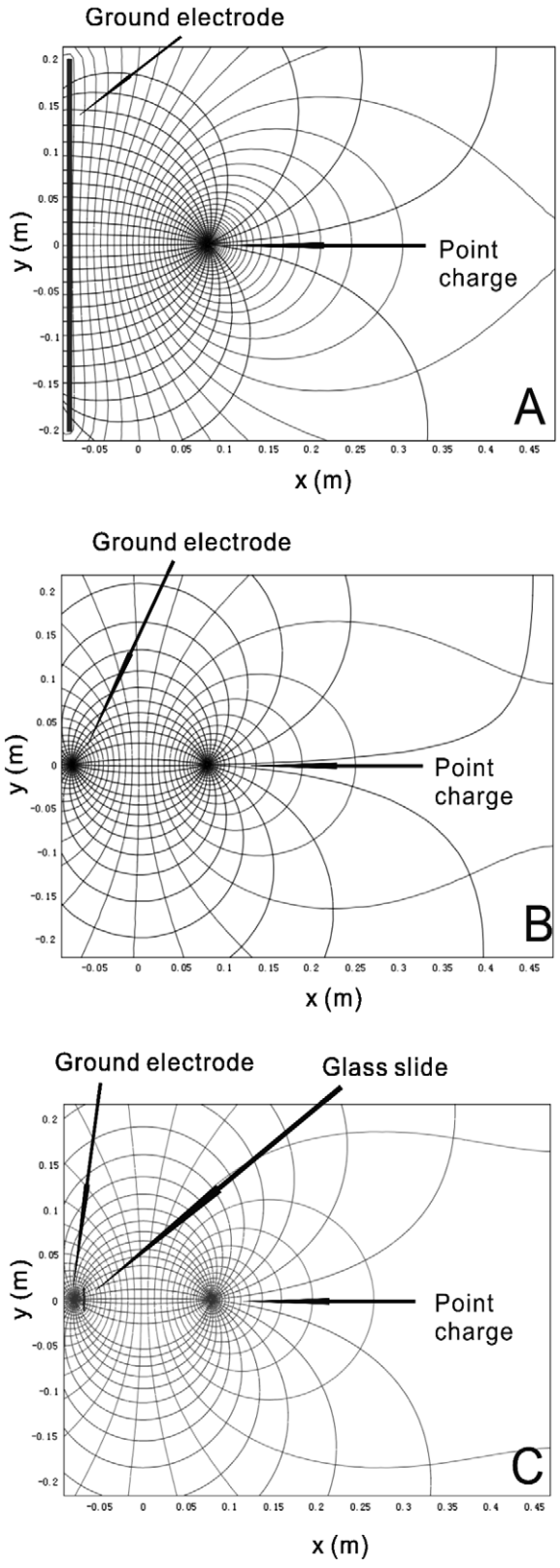

Fig. 7. The calculated equipotential lines and electrical field lines between a point charge and the ground electrodes with different size: (A) 40×40 cm^2, (B) 2×2 mm^2, (C) 2×2 mm^2 considering the effects of glass slide.

to understand the detailed formation mechanism of the aligned helical polymer nanofibers in this process.

4. Conclusions

In summary, aligned helical PCL nanofibers were prepared on tilted glass slides by using a unique setup. The helical structures were formed by the jet buckling when hitting the collector surface. The formation of the helical structures was dependant on the location and obliquity of tilted glass slide. The morphology of the collected fibers is sinuous folding at the low solution concentration of 3.5% and became helical with further increasing the solution concentration. The loop diameter of the helical structures is in the range of 6.9–14.9 μm depending on the solution concentration with the largest at the concentration of 5.8%. The 3-D helical structures were obtained at the high solution concentration of 10%. The electrical field lines were calculated for both the small and large area electrode, which shows that the small area electrode generates converging electrical field. It is inferred that the converging electrical field generated by the tip collector plays an important role in the aligning process of the helical structures by directing the fiber flight during electrospinning.

Acknowledgements

This work was supported by the NSFC (Grant No. 50572019), S&T program of Shenzhen government, and SRF for ROCS, SEM. J. Rafique is thankful to HEC and PAEC Pakistan for their support. We are grateful to Prof. Mingyu Li for help in taking the optical images.

References

[1] Bajpai V, Dai L, Ohashi T. Large-scale synthesis of perpendicularly aligned helical carbon nanotubes. J Am Chem Soc 2004;126:5070–1.
[2] Zhang HF, Wang CM, Buck EC, Wang LS. Synthesis, characterization, and manipulation of helical SiO_2 nanosprings. Nano Lett 2003;3:577–80.
[3] Kong XY, Wang ZL. Spontaneous polarization-induced nanohelixes, nanosprings, and nanorings of piezoelectric nanobelts. Nano Lett 2003;3:1625–31.
[4] Kessick R, Tepper G. Microscale polymeric helical structures produced by electrospinning. Appl Phys Lett 2004;84:4807–9.
[5] Shin, Kim SI, Kim SJ. Controlled assembly of polymer nanofibers: from helical springs to fully extended. Appl Phys Lett 2006;88:223109-1–9-3.
[6] Xin, Huang ZH, Yan EY, Zhang W, Zhao Q. Controlling poly(*p*-phenylene vinylene)/poly(vinyl pyrrolidone) composite nanofibers in different morphologies by electrospinning. Appl Phys Lett 2006;89:053101-1–1-3.
[7] Lin T, Wang HX, Wang XG. Self-Crimping bicomponent nanofibers electrospun from polyacrylonitrile and elastomeric polyurethane. Adv Mater 2005;17:2699–703.
[8] Reneker DH, Han T. Electrical bending and mechanical buckling instability in electrospinning jets. Mater Res Soc Symp Proc. 2007;948:0948–B07-01.
[9] Reneker DH, Yarin AL, Fong H, S.J.Koombhongse. Bending instability of electrically charged liquid jets of polymer solutions in electrospinning. J Appl Phys 2000;87:4531–47.
[10] Deitzel JM, Kleinmeyer JD, Hirvonen JK, Tan NCB. Controlled deposition of electrospun poly(ethylene oxide) fibers. Polymer 2001;42:8163–70.
[11] Theron A, Zumann E, Yarin AL. Electrostatic field-assisted alignment of electrospun nanofibres. Nanotechnology 2001;12:384–90.
[12] Fennessey SF, Farris RJ. Fabrication of aligned and molecularly oriented electrospun polyacrylonitrile nanofibers and the

mechanical behavior of their twisted yams. Polymer 2004;45: 4217–25.
[13] Katta P, Alessandro M, Ramsier RD, Chase GG. Continuous electrospinning of aligned polymer nanofibers onto a wire drum collector. Nano Lett 2004;4:2215–8.
[14] Sundaray B, Subramanian V, Natarajan TS, Xiang RZ, Chang CC, Fann WS. Electrospinning of continuous aligned polymer fibers. Appl Phys Lett 2004;84:1222–4.
[15] Sun DH, Chang C, Li S, Lin LW. Near-field electrospinning. Nano Lett 2006;6:839–42.
[16] Dersch R, Liu TQ, Schaper AK, Greiner A, Wendorff JH. Electrospun nanofibers: internal structure and intrinsic orientation. J Polym Sci Part A: Polym Chem 2003;41:545–53.
[17] Li D, Wang YL, Xia YN. Electrospinning of polymeric and ceramic nanofibers as uniaxially aligned arrays. Nano Lett 2003;3:1167–71.
[18] Dalton PD, Klee D, Moller M. Electrospinning with dual collection rings. Polymer 2005;46:611–4.
[19] Rafique, Yu J, Yu JL, Fang G, Wong KW, Zheng Z, et al. Electrospinning highly aligned long polymer nanofibers on large scale by using a tip collector. Appl Phys Lett 2007;91:063126-1–6-3.
[20] Fong H, Chun I, Reneker DH. Beaded nanofibers formed during electrospinning. Polymer 1999;40:4585–92.
[21] Yang QB, Li ZY, Hong YL, Zhao YY, Qiu SL, Wang C. Influence of solvents on the formation of ultrathin uniform poly(vinyl pyrrolidone) nanofibers with electrospinning. J Polym Sci Part B: Polym Phys 2004;42:3721–6.